

Arrival Time—Classical Parameter or Quantum Operator?

MohammadJavad Kazemi,^{1,*} MohammadHossein Barati,^{1,†}
Ghadir Jafari,^{2,‡} S. Shajidul Haque,^{3,4,§} and Saurya Das^{5,¶}

¹*Department of Physics, Faculty of Science, University of Qom, Qom, Iran*

²*Department of Physics Education, Farhangian University, P.O. Box 14665-889, Tehran, Iran*

³*Department of Mathematics & Applied Mathematics,
University of Cape Town, Cape Town, South Africa*

⁴*The National Institute for Theoretical and Computational Sciences,
Private Bag X1, Matieland, South Africa*

⁵*Department of Physics and Astronomy, University of Lethbridge, Lethbridge, Alberta T1K 3M4, Canada*

The question of how to interpret and compute arrival-time distributions in quantum mechanics remains unsettled, reflecting the longstanding tension between treating time as a quantum observable or as a classical parameter. Most previous studies have focused on the single-particle case in the far-field regime, where both approaches yield very similar arrival-time distributions and a semi-classical analysis typically suffices. Recent advances in atom-optics technologies now make it possible to experimentally investigate arrival-time distributions for entangled multi-particle systems in the near-field regime, where a deeper analysis beyond semi-classical approximations is required. Even in the far-field regime, due to quantum non-locality, the semi-classical approximation cannot generally hold in multi-particle systems. Therefore, in this work, two fundamental approaches to the arrival-time problem—namely, the time-parameter and time-operator approaches—are extended to multi-particle systems. Using these extensions, we propose a feasible two-particle arrival-time experiment and numerically evaluate the corresponding joint distributions. Our results reveal regimes in which the two approaches yield inequivalent predictions, highlighting conditions under which experiments could shed new light on distinguishing between competing accounts of time in quantum mechanics. Our findings also provide important insights for the development of quantum technologies that use entanglement in the time domain, including non-local temporal interferometry, temporal ghost imaging, and temporal state tomography in multi-particle systems.

I. INTRODUCTION

Consider a quantum particle with an initial wave function ψ evolving toward a detector waiting to observe it—arguably the simplest quantum experiment. When the experiment is repeated with the same initial state, the particle may be detected at different *times*, which can be measured with high precision [1–3]. How can one compute the *temporal* distribution of these detection events? Remarkably, even a century after the advent of quantum theory, there is still no universally agreed-upon answer to this fundamental question [4–14]. One of the main obstacles stems from the fact that, according to the principles of quantum theory, the distribution of any observable must be derived from a corresponding self-adjoint operator. Yet, in conventional quantum mechanics, time is not represented by a self-adjoint operator; instead, it is treated as a classical parameter that merely tracks the evolution of the wave function.

Within standard quantum theory, there appear to be only two possible approaches to addressing this arrival time problem. The first treats the arrival time as a quan-

tum observable in the usual sense, which requires introducing an appropriate arrival-time operator [14–24]. In the second approach, time is treated merely as a parameter, and without invoking an arrival time operator, the arrival time distribution is derived from other quantum observable distributions. This can be achieved by interpreting the experiment mentioned above as a continuous position measurement—i.e., a dense sequence of position measurements [4, 25–29]. Each approach faces significant challenges. On the one hand, as Pauli pointed out, no self-adjoint time operator satisfies $[\hat{H}, \hat{t}] = i\hbar$ when the Hamiltonian is bounded from below [6, 30]. On the other hand, without treating time as an operator, the most natural model of a *continuously waiting detector* forbids detection altogether, a manifestation of the quantum Zeno effect [4, 25, 26, 29, 31]. Several innovative approaches have been proposed to address these challenges, employing mathematical techniques and taking into account the specifics of real (rather than idealized) experiments [18, 21, 27, 32, 33] (see also Sec. II).

Most previous studies of the arrival-time problem have focused on simple cases, such as a free single particle in one-dimension, and have not yet been fully extended to more complex situations. Although approaches mentioned above are fundamentally distinct, their predictions often coincide for single-particle case under common experimental conditions—particularly in the regime where the detector is placed in the far-field (or scattering) limit.

* kazemi.j.m@gmail.com

† mohbarati14@gmail.com

‡ gh.jafari@cfu.ac.ir

§ shajid.haque@uct.ac.za

¶ saurya.das@uleth.ca

In fact, in this regime, a semi-classical approximation¹ is typically sufficient to estimate the arrival time distribution [7, 34, 37, 40, 41]. However, thanks to recent advances in atom optics—particularly the development of fast single-atom detectors [2, 42, 43], and generation and optical manipulation of entangled states [44–46]—it is now possible to explore entangled multi-particle systems in the near-field regime, where the semiclassical approximation breaks down, and a deeper analysis is required [7, 10]. Moreover, even in the far-field regime, due to quantum nonlocality, the semi-classical approximation cannot generally hold in multi-particle systems—see also [47, 48].

Accordingly, in this work, we extend two mentioned fundamental approaches to entangled multi-particle systems. Based on this extension, we propose and numerically simulate a simple two-particle arrival-time experiment that is feasible with current atom-interferometry technologies (see Fig. 1 and Section III for details). Our numerical results demonstrate that the arrival-time distributions predicted by the two approaches differ sufficiently to be experimentally distinguished. These findings not only shed new light on the foundations of quantum theory but also provide a more precise understanding of quantum phenomena in the time domain, which is crucial for progress in various quantum technologies that use entanglement in time domain, including non-local temporal interferometry [47, 49], temporal ghost imaging [42, 50], temporal state tomography [51, 52], and others [46, 53].

The rest of the paper is organized as follows. In Section II, we briefly review the two aforementioned arrival-time approaches and extend them to two-particle systems. In Section III, we present and compare the simulation results for the two-particle distributions based on these approaches. Finally, in Section IV, we summarize the findings and discuss future prospects.

II. THEORETICAL FRAMEWORKS

In this section, we review two main approaches to the arrival-time problem within the standard quantum theory framework—the *time-operator* and the *time-parameter* approaches—and extend them to entangled multi-particle systems, with particular emphasis on the two-particle case.

A. Arrival Time Operator

The earliest attempts to address the arrival-time problem within the framework of standard quantum theory date back to the early 1960s, with pioneering works by Aharonov and Bohm [54] and, independently, by Paul [55]. These studies began with a symmetric quantization of the classical expression for the arrival time. In the one-dimensional case, the classical arrival time of a freely moving particle of mass m , initially located at x_0 with momentum p_0 , as it travels to a point $x = L$, is given by

$$t = m(L - x_0)/p_0, \quad (1)$$

The symmetric quantization of this classical expression yields the following arrival time operator [5]:

$$\hat{t}_{AB} = mL \hat{p}^{-1} - \frac{m}{2} (\hat{p}^{-1} \hat{x} + \hat{x} \hat{p}^{-1}), \quad (2)$$

Here, \hat{x} and $\hat{p} = -i \partial/\partial x$ represent the standard position and momentum operators, respectively, while \hat{t}_{AB} is referred to as the Aharonov-Bohm time operator. This operator satisfies the canonical commutation relation with the free Hamiltonian operator, $[\hat{t}_{AB}, \hat{p}^2/2m] = i\hbar$, which has been used to derive the energy-time uncertainty relation [56, 57]. However, while \hat{t}_{AB} is Hermitian (or symmetric, as referred to in mathematical contexts), it is not a self-adjoint operator [58]—a result consistent with Pauli’s theorem [30].

The non-self-adjoint nature of \hat{t}_{AB} arises from the singularity at $p = 0$ in its momentum representation, $\hat{t}_{AB} \rightarrow (i\hbar m/2)(p^{-2} - 2p^{-1}\partial_p)$ [58]. Grot, Rovelli, and Tate addressed this singularity in Eq. (2) by introducing a symmetric regularization and derived the corresponding arrival-time probability density using the standard Born rule [57], expressed as [56, 58]:

$$\Pi(t|x = L) = |\langle t|\psi_0 \rangle|^2, \quad (3)$$

where $|t\rangle$ denotes the eigenstate of the arrival-time operator \hat{t}_{AB} corresponding to the temporal eigenvalue t . In the momentum representation, the arrival-time probability density takes the form

$$\Pi(t|x=L) = \frac{1}{2\pi\hbar} \sum_{\alpha=\pm} \left| \int_{-\infty}^{\infty} dp \theta(\alpha p) \sqrt{\frac{|p|}{m}} \tilde{\psi}_t(p) e^{\frac{iLp}{\hbar}} \right|^2, \quad (4)$$

where $\theta(\cdot)$ is the Heaviside step function, and $\tilde{\psi}_t(p)$ is the momentum-space wave function related to the initial state by $\tilde{\psi}_t(p) = \tilde{\psi}_0(p) \exp(-itp^2/2m\hbar)$. Extensions of equations (2) and (4) to include interaction potentials have been explored in various studies [8, 16–19, 32, 59, 60]. These works demonstrate that the non-self-adjoint nature of the free arrival-time operator can be resolved through spatial confinement as well [19, 61]. Specifically, the Eq. (4) can be obtained as the limiting case of the arrival-time distribution in a confining box

¹ In this approximation, particles are assumed to follow classical trajectories, and the arrival time distribution is estimated from the quantum momentum distribution [7, 34–37]. However, it should be noted that due to the quantum backflow effect [38], even in free space, the time evolution of the quantum position probability density is not consistent with the underlying uniform motion, especially in near-field regime [39].

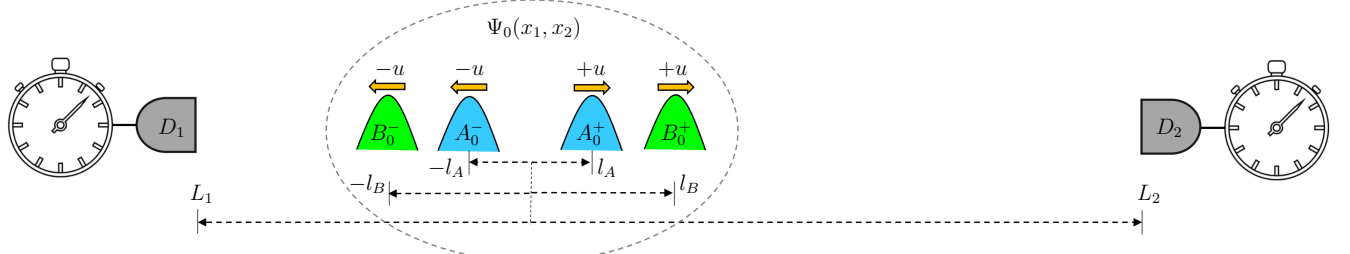


FIG. 1. **Schematic diagram of the proposed setup.** In this setup, two entangled particles are prepared in the initial entangled state $\Psi_0(x_1, x_2)$, composed of four Gaussian wave packets, as described in Eq. (26). The left detector D_1 and the right detector D_2 are waiting to measure the arrival times of the left-moving and the right-moving particles, respectively.

as the box length approaches infinity [18]. Additionally, recent studies have derived the distribution (4) from a space-time-symmetric extension of non-relativistic quantum mechanics [15, 62]. The distribution (4) and its generalizations in the presence of interaction potentials have been referred to as the "standard arrival-time distribution" by several authors [6, 8, 63–65].

We now generalize this standard arrival-time distribution to the two-particle case. Fig. 1 illustrates a schematic diagram of a typical experimental setup designed to measure the arrival times of two entangled particles. The setup consists of a source that produces pairs of entangled particles, such as helium atoms. The particles propagate in opposite directions toward two detectors

located at distances L_1 and L_2 . These detectors are configured to precisely record the arrival times of the particles, denoted by t_1 and t_2 . The goal is to compute the joint two-particle arrival-time probability density, $\Pi(t_1, t_2)$, based on the particles' initial state $|\Psi_0\rangle$. In this regard, we generalize the standard one-particle arrival-time probability density to the two-particle case in the usual way, as follows:

$$\Pi(t_1, t_2 | x_1 = L_1, x_2 = L_2) = |\langle t_1, t_2 | \Psi_0 \rangle|^2, \quad (5)$$

where $|t_1, t_2\rangle$ is defined as the tensor product of the eigenstates of the one-particle arrival-time operators, i.e., $|t_1, t_2\rangle = |t_1\rangle_{L_1} \otimes |t_2\rangle_{L_2}$. Accordingly, in the momentum representation, the two-particle arrival-time probability density is given by

$$\Pi(t_1, t_2 | L_1, L_2) = \sum_{\alpha_1, \alpha_1 = \pm} \frac{1}{(2\pi\hbar)^2} \left| \int dp_1 dp_2 \tilde{\Psi}_0(p_1, p_2) \theta(\alpha_1 p_1) \theta(\alpha_2 p_2) \sqrt{\frac{p_1}{m_1}} \sqrt{\frac{p_2}{m_2}} e^{-\frac{i}{\hbar}(\frac{p_1^2 t_1}{2m_1} + \frac{p_2^2 t_2}{2m_2})} e^{\frac{i}{\hbar}(p_1 L_1 + p_2 L_2)} \right|^2. \quad (6)$$

As expected, when the initial state of the system is separable, the two-particle arrival-time distribution reduces to a product of the single-particle distributions:

$$\Pi(t_1, t_2 | L_1, L_2) = \Pi_1(t_1 | L_1) \Pi_2(t_2 | L_2). \quad (7)$$

However, when the particles are entangled, the joint two-particle arrival-time distribution exhibits correlations. In fact, using the *two-time wave function* [66], the two-particle standard arrival-time distribution can be expressed as the following non-local form:

$$\begin{aligned} \Pi(t_1, t_2 | L_1, L_2) &= \sum_{\alpha_1, \alpha_1 = \pm} \frac{\hbar^2}{(32\pi)^2} \times \\ &\left| \int K(x_1, x_2) \left(\Psi_{t_1, t_2}(x_1, x_2) - \Psi_{t_1, t_2}(L_1, L_2) \right) dx_1 dx_2 \right|^2, \quad (8) \end{aligned}$$

where the two-time wave function is defined as [66, 67]:

$$\Psi_{t_1, t_2}(x_1, x_2) = \langle x_1, x_2 | e^{-\frac{i}{\hbar} \hat{H}_1 t_1} e^{-\frac{i}{\hbar} \hat{H}_2 t_2} | \Psi_0 \rangle, \quad (9)$$

and the kernel $K(x_1, x_2)$ is given by

$$K(x_1, x_2) = \left(\frac{1 + \alpha_1 \text{sgn}(x_1 - L_1)}{|x_1 - L_1|^{3/2}} \right) \left(\frac{1 + \alpha_2 \text{sgn}(x_2 - L_2)}{|x_2 - L_2|^{3/2}} \right).$$

B. Arrival time experiment as a sequence of position measurement

As previously discussed in the Introduction I, by treating time as a classical parameter rather than as a quantum observable, the most natural approach to modeling arrival-time experiments is to describe them as a sequence of position measurements. For a single-particle arrival-time experiment, the procedure is as follows: a

particle is released from a specified region at time $t = 0$, evolving unitarily toward the detector, and within the detection region, repeated instantaneous projective measurements are conducted at regular time intervals τ to ascertain whether the particle has arrived. The experiment is finished as soon as the particle is detected for the first time. If the particle is detected at the n th measurement, the particle's time of arrival into the detection region is taken to be $t = n\tau$ (or, more precisely, between $t - \tau$ and t). In a few words, the detector outputs can be represented as a binary string of length n , describing detection success: “no, no, …, no, yes”. It is important to note that the probability of first detection at the n th measurement is not the same as the probability of detection in $t = n\tau$ given no previous measurements. This is because, after each *null* measurement—i.e., a measurement without particle detection—the wave function is projected outside the detection region, according to the standard von Neumann measurement postulate. Consequently, the unitary evolution of the wave function is interrupted by a sequence of projections made at regular time intervals τ . Therefore, using the Born rule, the probability of the first arrival at the n th measurement is given by [25, 26, 28, 29, 68]:

$$\tau\Pi_n = (1 - \mathcal{P}_1)(1 - \mathcal{P}_2) \cdots (1 - \mathcal{P}_{n-1})\mathcal{P}_n, \quad (10)$$

where \mathcal{P}_k is defined as

$$\mathcal{P}_k = \int_{\mathcal{D}} |\psi_k(x)|^2 dx, \quad (11)$$

in which \mathcal{D} is the active domain of the detector, and the wave function at $t = k\tau$ is given by

$$\psi_k(x) = N_k \langle x | e^{-i\hat{H}\tau/\hbar} \left(\hat{\hat{P}} e^{-i\hat{H}\tau/\hbar} \right)^{k-1} | \psi_0 \rangle, \quad (12)$$

where \hat{H} is the (free) Hamiltonian, $\hat{\hat{P}}$ is the projection operator corresponding to the null measurements, defined as $\hat{\hat{P}} = \mathbb{1} - \int_{\mathcal{D}} dx |x\rangle\langle x|$, and N_k is the normalization constant—after each projection, the wave function must be re-normalized. Beyond the arrival-time problem, such non-unitary quantum dynamics of a system subjected to repeated monitoring have garnered significant attention recently, largely due to the growing interest in quantum information (see, e.g., [28, 69–71]).

Continuous monitoring of this kind—where the time interval between measurements is taken to zero—leads to a surprising outcome: the quantum particle is never detected, a phenomenon known as the quantum Zeno effect [29, 31, 72]. This phenomenon arises from the general properties of quantum dynamics, which imply a quadratic behavior in the survival probability at short time scales [73–75]; when $\tau \rightarrow 0$, the squared norms of the wave-function in the detection region tend to zero as quickly as $o(\tau^2)$, and so the total probability of particle detection in a fixed time interval $[0, T]$ vanishes as $o(\tau)$ [4]. In fact, the limit $\tau \rightarrow 0$ represents an infinitely fast and sensitive detector, and the quantum Zeno effect demonstrates that such a perfect detection screen, if it existed, could not work—Its unlimited sensitivity would cause the complete reflection of the wave packet rather than its detection. In contrast, it appears that any real detection screens possess finite sensitivity and a corresponding finite “awareness” time τ . This finite sensitivity results in a small but non-zero probability that (wave function of) the particle may pass through the screen before being detected, thereby ensuring a non-zero detection probability.

Let us extend this time-parameter approach to the two-particle case. While the generalization follows naturally from the principles of quantum theory, it is not trivial. The total wave function of the particles evolves according to the Schrödinger equation in the two-particle space. However, when a measurement is performed on one part of the system, the wave function must be projected onto the subspace corresponding to the measurement outcome. In our setup, two detectors are waiting for particle arrivals. This *waiting* is modeled as a sequence of measurements performed at time intervals of τ . At each time step, if one or both detectors register (or fail to register) a particle, the total wave function is projected onto a subspace consistent with the measurement result. Suppose that during the first n time steps, neither detector detects a particle. In each of these steps, the wave function is projected onto the subspace corresponding to no detection. When, at a later time step, one detector registers a particle while the other does not, the wave function is then projected onto the corresponding subspace; specifically, when the first particle is *absorbed* by a macroscopic detector, the two-particle wave function effectively reduces to a single-particle wave function. Therefore, the two-particle joint arrival time distribution, i.e., the joint probability of detecting particle 1 at $t_1 \in [(n-1)\tau, n\tau]$ and particle 2 at $t_2 \in [(m-1)\tau, m\tau]$, is given by

$$\tau^2\Pi_{n,m} = \begin{cases} (\bar{\mathcal{P}}_1 \dots \bar{\mathcal{P}}_{n-1}) \tilde{\mathcal{P}}_n^{(1)} (\bar{\mathcal{P}}_{n,n+1}^{(2)} \dots \bar{\mathcal{P}}_{n,m-1}^{(2)}) \mathcal{P}_{n,m}^{(2)} & n < m \\ (\bar{\mathcal{P}}_1 \dots \bar{\mathcal{P}}_{n-1}) \mathcal{P}_n & n = m \\ (\bar{\mathcal{P}}_1 \dots \bar{\mathcal{P}}_{m-1}) \tilde{\mathcal{P}}_m^{(2)} (\bar{\mathcal{P}}_{m,m+1}^{(1)} \dots \bar{\mathcal{P}}_{m,n-1}^{(1)}) \mathcal{P}_{m,n}^{(1)} & n > m \end{cases} \quad (13)$$

where, using the born rule, the probabilities are given as

$$\mathcal{P}_k = \int_{\mathcal{D}_1} dx_1 \int_{\mathcal{D}_2} dx_2 |\langle x_1, x_2 | \Psi_k \rangle|^2, \quad (14)$$

$$\bar{\mathcal{P}}_k = \int_{\bar{\mathcal{D}}_1} dx_1 \int_{\bar{\mathcal{D}}_2} dx_2 |\langle x_1, x_2 | \Psi_k \rangle|^2, \quad (15)$$

$$\tilde{\mathcal{P}}_k^{(1)} = \int_{\mathcal{D}_1} dx_1 \int_{\bar{\mathcal{D}}_2} dx_2 |\langle x_1, x_2 | \Psi_k \rangle|^2, \quad (16)$$

$$\tilde{\mathcal{P}}_k^{(2)} = \int_{\bar{\mathcal{D}}_1} dx_1 \int_{\mathcal{D}_2} dx_2 |\langle x_1, x_2 | \Psi_k \rangle|^2, \quad (17)$$

$$\mathcal{P}_{k,k+l}^{(i)} = \int_{\mathcal{D}_i} dx_i |\langle x_i | \psi_{k,l}^{(i)} \rangle|^2, \quad (18)$$

$$\bar{\mathcal{P}}_{k,k+l}^{(i)} = \int_{\bar{\mathcal{D}}_i} dx_i |\langle x_i | \psi_{k,l}^{(i)} \rangle|^2. \quad (19)$$

in which \mathcal{D}_i represents the active domain of the i th detector: i.e., in our setup, $\mathcal{D}_1 = (-\infty, L_1]$, $\mathcal{D}_2 = [L_2, \infty)$, and $\bar{\mathcal{D}}_i = \mathbb{R} - \mathcal{D}_i$. The two-particle wave function after no detection of either particle at time step k is given by

$$|\Psi_k\rangle = N_k e^{-i\hat{H}\tau/\hbar} \left(\hat{\hat{P}} e^{-i\hat{H}\tau/\hbar} \right)^{k-1} |\Psi_0\rangle, \quad (20)$$

and the one-particle wave functions after a particle is detected at time step k by one detector while the other detector has not yet recorded a detection event at time step $k+l$, are given by

$$|\psi_{k,l}^{(1)}\rangle = N_{kl}^{(1)} e^{-i\hat{H}_1\tau/\hbar} \left(\hat{\hat{P}}^{(1)} e^{-i\hat{H}_1\tau/\hbar} \right)^{l-1} \hat{P}^{(2)} |\Psi_k\rangle, \quad (21)$$

$$|\psi_{k,l}^{(2)}\rangle = N_{kl}^{(2)} e^{-i\hat{H}_2\tau/\hbar} \left(\hat{\hat{P}}^{(2)} e^{-i\hat{H}_2\tau/\hbar} \right)^{l-1} \hat{P}^{(1)} |\Psi_k\rangle, \quad (22)$$

where \hat{H} is the total Hamiltonian of the two-particle system, \hat{H}_1 and \hat{H}_2 are the single-particle Hamiltonians, N_k and $N_{kl}^{(i)}$ are normalization constants, and $\hat{\hat{P}}$, $\hat{P}^{(i)}$, and $\hat{P}^{(i)}$ are the two-particle and one-particle projection operators, which are given by:

$$\hat{\hat{P}} = \int_{\bar{\mathcal{D}}_1} dx_1 \int_{\bar{\mathcal{D}}_2} dx_2 |x_1, x_2\rangle \langle x_1, x_2|, \quad (23)$$

$$\hat{P}^{(i)} = \int_{\bar{\mathcal{D}}_i} dx_i |x_i\rangle \langle x_i|, \quad (24)$$

$$\hat{P}^{(i)} = \int_{\mathcal{D}_i} dx_i |x_i\rangle \langle x_i|. \quad (25)$$

III. NUMERICAL SIMULATION AND RESULTS

In this section, we numerically study the differences between the two mentioned arrival-time approaches—namely, the time-operator and time-parameter frameworks—in a minimal two-particle arrival-time experiment. The experimental configuration is schematically illustrated in Fig. (1). In this setup, a pair of entangled particles is prepared near the origin with an initial wave function composed of two double wave packets—one propagating to the right and the

other to the left. On the left side at $x = L_1$ and on the right side at $x = L_2$, there are two particle detectors waiting to detect the particles and record the detection times. By repeating the experiment many times, the joint two-particle arrival-time distribution can be reconstructed from the ensemble of recorded arrival times.

The initial wave function can be considered as follows:

$$\Psi_0(x_1, x_2) = \frac{1}{\sqrt{2}} (A_0^+(x_1) A_0^-(x_2) + B_0^+(x_1) B_0^-(x_2)), \quad (26)$$

where

$$A_0^\pm(x) = G(x; \sigma_0, \pm l_A, \pm u), \quad (27)$$

$$B_0^\pm(x) = G(x; \sigma_0, \pm l_B, \pm u), \quad (28)$$

and G is a Gaussian wave function as follows:

$$G(x; \sigma, l, u) = N e^{-(x-l)^2/4\sigma^2 + i u (x-l)/\hbar}. \quad (29)$$

This kind of entangled Gaussian state is practical for implementation in quantum technologies because such states can be readily produced and reliably controlled [44, 47, 76].

Using Eq. (6) together with Eq. (26), we plot in the left column of Fig. 2 the joint arrival-time probability density within the time-operator framework. In this figure, the scatter plots are generated using 10^5 sample points, and the parameters have been chosen as $\sigma_x = 10^{-6}$ (m), $u_x = 0.1$ (m/s), $l_A = 8 \times \sigma_0$ (m), $l_B = 12 \times \sigma_0$ (m) and $m_1 = m_2 = 6.646 \times 10^{-27}$ (kg). These values are in agreement with the proposed setup in reference [77] in which colliding Helium-4 atoms have been used for producing the initial entangled state [78]—The double-double-slit setup introduced in the reference [77] can be utilized to produce our initial entangled wave function. Furthermore, analogous initial entangled states can be realised and precisely controlled in optical trapping configurations, providing an alternative experimental platform in which the degree of entanglement can be systematically engineered and the arrival-time distribution can be accurately measured [44].

In order to compute the arrival-time distribution within the time-parameter framework, one must first determine the time evolution of the initial wave function (26), taking into account the detector's back-effect. Since the free two-particle Hamiltonian is separable, the time evolution of this wave function can be found from the time evolution of each single-particle wave packet as follows:

$$\Psi_k(x_1, x_2) = N_k (A_k^+(x_1) A_k^-(x_2) + B_k^+(x_1) B_k^-(x_2)), \quad (30)$$

in which N_k is the normalization constant, $A_k^\pm(x)$ and $B_k^\pm(x)$ are constructed from the time evolution of the associated initial Gaussian wave functions—according to Eq. (12)—as follows:

$$A_k^\pm(x) = N_k^{A^\pm} \langle x | e^{-i\hat{H}\tau/\hbar} \left(\hat{\hat{P}} e^{-i\hat{H}\tau/\hbar} \right)^{k-1} | A_0^\pm \rangle, \quad (31)$$

$$B_k^\pm(x) = N_k^{B^\pm} \langle x | e^{-i\hat{H}\tau/\hbar} \left(\hat{\hat{P}} e^{-i\hat{H}\tau/\hbar} \right)^{k-1} | B_0^\pm \rangle, \quad (32)$$

where, $N_k^{A\pm}$ and $N_k^{B\pm}$ represent normalization constants and, $|A_0^\pm\rangle$ and $|B_0^\pm\rangle$ are vector states associated with the initial wave packets $A_0^\pm(x)$ and $B_0^\pm(x)$, respectively. Moreover, according to Eq (21) and Eq (22), the single-particle wave functions are given by

$$\psi_{k,l}^{(1)}(x_1) = N_{kl}^{(1)} (\alpha_k^- A_{k+l}^+(x_1) + \beta_k^+ B_{k+l}^+(x_1)), \quad (33)$$

$$\psi_{k,l}^{(2)}(x_2) = N_{kl}^{(2)} (\alpha_k^+ A_{k+1}^-(x_2) + \beta_k^- B_{k+1}^-(x_2)), \quad (34)$$

where,

$$\alpha_k^+ = \int_{\mathcal{D}_1} A_k^+(x_1) dx_1, \quad (35)$$

$$\alpha_k^- = \int_{\mathcal{D}_2} A_k^-(x_2) dx_2, \quad (36)$$

$$\beta_k^+ = \int_{\mathcal{D}_1} B_k^+(x_1) dx_1, \quad (37)$$

$$\beta_k^- = \int_{\mathcal{D}_2} B_k^-(x_2) dx_2. \quad (38)$$

Using the wave functions (30), (33), and (34), one can numerically compute the joint arrival-time probability density in the time-parameter approach, which is given in Eq.(13). It is worth noting that the numerical simulation of Eq. (13) is substantially more demanding than the corresponding single-particle case, Eq. (10). The increased computational complexity arises not only from the higher dimensionality of the problem, but also from the larger number of integrals that must be evaluated—particularly when τ is small compared to the simulation time T . To address these challenges, we developed a computationally efficient Python implementation of the Crank-Nicolson method for solving the Schrödinger equation, as well as a Simpson-rule integration scheme, using Numba-compatible functions [79] to speedup the numerical computations. As a result, in the right column of the Fig. 2, the joint arrival-time distribution Eq. (13), is plotted. In this column, the temporal detection resolution is chosen as $\tau = 10^{-6}$ s, and the parameters of the initial wave function are the same as one described earlier for the left-column. Moreover, in all panels of this figure, the position of the right detector is fixed at $L_2 = 200\sigma_0$, while the position of the left detector varies from the far-field to the near-field regime—In panels (a)-(b), (c)-(d), and (e)-(f), the left detector is placed at $L_1 = -100\sigma_0$, $L_1 = -50\sigma_0$, and $L_1 = -20\sigma_0$, respectively.

The numerical results allow for a detailed comparison of the two competing formulations of arrival-time in quantum mechanics. Interestingly enough, although these approaches are fundamentally different, they yield nearly identical distributions in the far-field regime, as seen in the top panels of Fig. 2. In this regime, both approaches predict non-classical *multi-particle interference in arrival time*, a quantum phenomenon that has recently been predicted for atoms [47] and observed using photons [80–83] in conceptually similar setups.

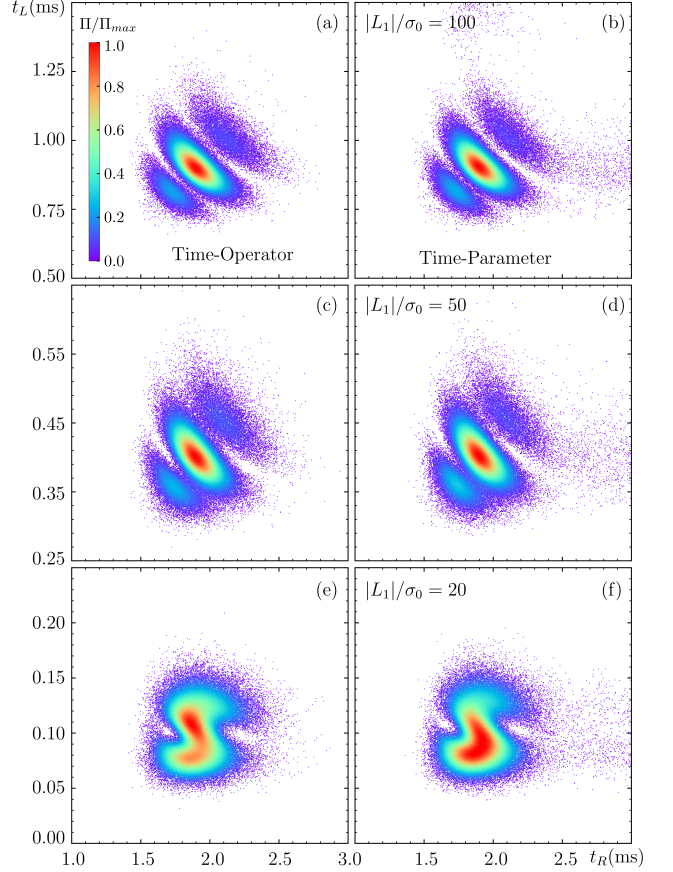


FIG. 2. **Comparing arrival-time distributions in the near-field and far-field regimes.** Panels (a), (c), and (e) (left column) represent two-particle arrival-time distributions resulted from the time-operator approach, whereas panels (b), (d), and (f) (right column) display the corresponding distributions computed using the time-parameter approach. The rows indicate different left-detector positions, arranged from the far-field at the top to the near-field regime at the bottom. As seen, the two approaches differ more clearly in the near-field regime. Each scatter plot is generated using 10^5 sample points. The parameters of the initial wave function are chosen as $\sigma_0 = 10^{-6}$ m, $u = 10^{-1}$ m/s, $l_A = 8\sigma_0$, and $l_B = 12\sigma_0$. The right detector is placed at $L_2 = 200\sigma_0$. In panels (a)-(b), (c)-(d), and (e)-(f), the left detector is placed at $L_1 = -100\sigma_0$, $L_1 = -50\sigma_0$, and $L_1 = -20\sigma_0$, respectively. All the distributions are computed for Helium atoms with mass $m = 6.64 \times 10^{-27}$ kg. In Each panel, the colormap is normalized to Π_{max} , the maximum of arrival time probability density. In the right-column plots, the detection temporal resolution is fixed to be $\tau = 10^{-6}$ s.

In contrast, in the near-field regime—shown in the bottom panels of Fig. 2—the shapes of the resulting distributions differ noticeably, and thus the distinction between the two approaches becomes more pronounced. For example, the two approaches yield different mean arrival times in this regime. Consequently, this regime provides a promising setting for performing measurements that could determine which aforementioned arrival-time

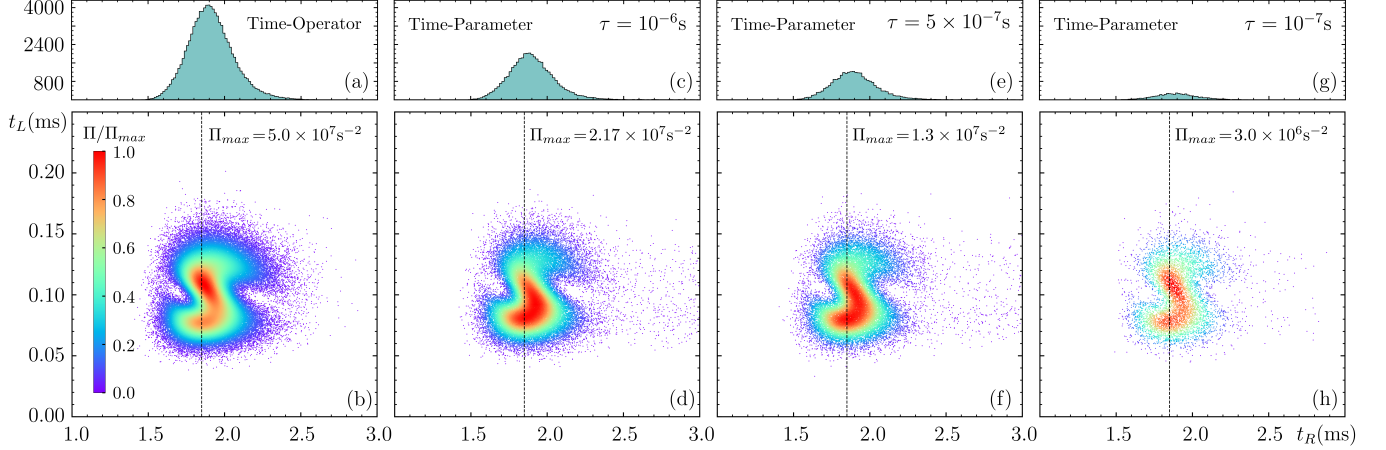


FIG. 3. **Detector temporal resolution effect on the arrival-time distribution.** Panel (b) shows the two-particle arrival-time distribution obtained from the arrival time-operator approach, with its corresponding marginal shown in panel (a). Panels (d), (f), and (h) show the two-particle arrival-time distributions obtained from the time-parameter approach, with detector temporal resolutions $\tau = 10^{-6}\text{s}$, $\tau = 5 \times 10^{-7}\text{s}$, and $\tau = 10^{-7}\text{s}$, respectively—their corresponding marginals appear in panels (c), (e), and (g). In all panels, the right detector is placed at $L_2 = 200\sigma_0$ and the left detector at $L_1 = -20\sigma_0$. The distributions are computed for Helium atoms using the same initial wave-function parameters as in Fig. (2). All colormaps are normalized to the maximum arrival-time probability density of the time-operator distribution. In the time-parameter approach, higher temporal resolution lowers the total detection probability due to the quantum Zeno effect, reflected in the fewer sampled points in panels (d), (f), and (h).

framework, if any, is compatible with experimental data. Moreover, even in the far-field regime, the arrival-time distributions obtained from the time-parameter approach exhibit small tails, which can be used to experimentally distinguish between the two approaches. However, observing this feature is experimentally challenging due to its very small magnitude.

Understanding how the arrival-time distribution in the time-parameter approach depends on the detection temporal resolution is essential for optimizing experimental settings to enable a meaningful comparison between the two approaches. In this regard, in Fig. 3, we plot the arrival-time distribution for several values of the detection temporal resolution, where other parameter values are chosen the same as in the bottom panels of Fig. 2. As expected from the quantum Zeno effect, increasing the detection frequency suppresses the total detection probability, a behavior reflected in the reduced number of recorded detection events as τ decreases—see also the top panels of Fig. 3. This result is in agreement with previous studies that numerically investigate the time-parameter approach with finite τ for a single particle in a 1D lattice [26, 29]. Furthermore, Fig. 3 indicates that although the total detection probability decreases, the difference between the shapes of the distributions obtained from the two arrival-time approaches becomes less pronounced as the detection resolution increases. For a more detailed examination, Fig. 4 presents the conditional arrival-time distribution at the left detector, $\Pi(t_L|t_R)$, corresponding to a slice of the joint distributions in Fig. 3 indicated by vertical lines. This figure demonstrates that decreasing

τ reduces the discrepancy between the predictions of the time-parameter and time-operator approaches, suggesting that very fine temporal monitoring may diminish the distinguishability of the two frameworks.

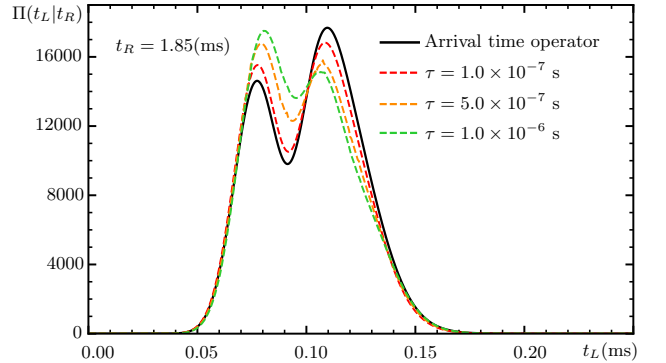


FIG. 4. **Conditional arrival-time probability density.** The plot shows the *normalized* conditional arrival-time probability densities for the left detector, $\Pi(t_L|t_R)$, evaluated at the fixed right detection-time $t_R = 1.85\text{ ms}$ (corresponding to the vertical lines in Fig. 3). The solid curve depicts the arrival-time probability density obtained from the time-operator approach, while the dashed curves represent the results from the time-parameter approach. As seen, the results of two approaches coincide, when τ decrease.

The simulation results presented in Figs. 2, 3 and 4 clearly demonstrate that a detector with microsecond temporal resolution—such as those reported in Refs.

[3, 84]—is fully sufficient to unambiguously discriminate between the two approaches. Given that the characteristic temporal scale of the distributions is on the order of $100\mu\text{s}$, such resolution enables accurate reconstruction of the full temporal profiles. Finally, it is important to remark that the preparation of the required initial wave function is readily achievable with existing atom-optics technologies, including established methods for the generation, optical cooling, and manipulation of entangled atoms [44, 46, 85, 86].

IV. SUMMARY AND OUT-LOOK

In this work, we extend two distinct treatments of the arrival-time problem within standard quantum theory to multi-particle systems and propose an experimentally feasible scheme that can discriminate between their predictions. Numerical simulations performed across a broad region of parameter space show that, although the two approaches generally yield nearly identical results—most notably in the far-field regime—there exists an experimentally accessible domain in which their predictions diverge substantially. This deviation is sufficiently large to make the two formulations experimentally distinguishable using current atom-interferometry techniques. Moreover, by examining the dependence of the arrival-time distributions on the detection resolution, we find that although the time-parameter approach exhibits a suppressed detection probability near the Zeno regime, the discrepancy between the two approaches nevertheless decreases as τ is reduced.

Beyond the fundamental questions addressed here, our results also have direct implications for practical applications in atom optics that rely on entangled particles, including atomic ghost imaging [42, 50], entanglement-enhanced gravimetry [53], and related quantum-sensing technologies [51, 52]. A detailed analysis of these applications is left for future work. Nevertheless, it is important to emphasize that realistic implementations will require extending the present studies to interacting multi-particle systems subject to external gravitational fields. Such extensions are computationally demanding and will require the development of optimized numerical methods, thereby defining an important direction for future research.

Moreover, at least for applications in quantum optics, it is essential to extend these approaches for relativistic particles, particularly photons. This represents an important research direction, as the measurement of photon arrival-time distributions using state-of-the-art ultra-fast detectors [1, 87, 88] forms a cornerstone of modern quantum technologies—for example see [83, 89, 90]. At a fundamental level, however, this remains a challenging problem. While a natural relativistic generalization of the Aharonov–Bohm time-of-arrival operator has been proposed [23, 91], it is defined in terms of a position operator, whose definition in a relativistic context remains controversial [92–94]. Similarly, the time-parameter approach relies on a well-defined position probability density, which is also problematic in the relativistic regime and lacks a universally accepted definition [95–99], at least for bosons. Recently, some of the present authors have developed a framework for quantum mechanics that does not rely on a self-adjoint position operator [100, 101], offering a promising avenue to address these issues. Detailed investigations of relativistic extensions and their implications for photon-based quantum technologies are left for future works.

Finally, it is important to remark that in principle it is possible that, in a sufficiently accurate experiment, neither mention approach will match the measured data, indicating the need for a more realistic modeling of the detection process. This possibility may, in turn, bring us closer to an experimental investigation of the *measurement problem* [102]. In this regard, comparing our results with arrival-time predictions in alternative quantum theories—particularly continuous-collapse models [103, 104] and Bohmian mechanics [47, 105]—constitutes an important direction for future work.

ACKNOWLEDGEMENT

The authors acknowledge access to the high-performance computing cluster at University of Qom, which made the numerical simulations in this work possible. SSH is supported in part by the by the “Quantum Technologies for Sustainable Development” project from the National Institute for Theoretical and Computational Sciences (NITheCS). M.K would like to thank Mohammad Khorrami for insightful discussion.

-
- [1] B. Korzh, Q.-Y. Zhao, J. P. Allmaras, S. Frasca, T. M. Autry, E. A. Bersin, A. D. Beyer, R. M. Briggs, B. Bumble, M. Colangelo, *et al.*, *Nature Photonics* **14**, 250 (2020).
- [2] M. Keller, M. Kotyrba, F. Leupold, M. Singh, M. Ebner, and A. Zeilinger, *Physical Review A* **90**, 063607 (2014).
- [3] C. Kurtsiefer and J. Mlynek, *Applied Physics B* **64**, 85 (1996).
- [4] B. Mielnik, *Foundations of physics* **24**, 1113 (1994).
- [5] J. Muga and C. Leavens, *Physics Reports* **338**, 353 (2000).
- [6] G. Muga, R. S. Mayato, and I. Egusquiza, *Time in quantum mechanics*, Vol. 734 (Springer Science & Business Media, 2007).
- [7] N. Vona, G. Hinrichs, and D. Dürr, *Phys. Rev. Lett.* **111**, 220404 (2013).
- [8] S. Das and M. Nöth, *Proceedings of the Royal Society A* **477**, 20210101 (2021).

- [9] S. Das and W. Struyve, *Phys. Rev. A* **104**, 042214 (2021).
- [10] A. Ayatollah Rafsanjani, M. Kazemi, A. Bahrampour, and M. Golshani, *Communications Physics* **6**, 195 (2023).
- [11] S. Roncallo, K. Sacha, and L. Maccone, *Quantum* **7**, 968 (2023).
- [12] S. Goldstein, R. Tumulka, and N. Zanghì, *Scientific reports* **14**, 3775 (2024).
- [13] A. Drezet, *Symmetry* **16**, 1325 (2024).
- [14] L. Maccone and K. Sacha, *Physical Review Letters* **124**, 1110402 (2020).
- [15] R. E. Araújo, R. Ximenes, and E. O. Dias, *Physical Review A* **109**, 012221 (2024).
- [16] P. C. M. Flores and E. A. Galapon, *Phys. Rev. A* **99**, 042113 (2019).
- [17] E. A. Galapon, *Phys. Rev. Lett.* **108**, 170402 (2012).
- [18] E. A. Galapon, F. Delgado, J. G. Muga, and I. n. Egusquiza, *Phys. Rev. A* **72**, 042107 (2005).
- [19] E. A. Galapon, R. F. Caballar, and R. T. B. Jr, *Phys. Rev. Lett.* **93**, 180406 (2004).
- [20] J. Kijowski, *Phys. Rev. A* **59**, 897 (1999).
- [21] N. Grot, C. Rovelli, and R. S. Tate, *Physical Review A* **54**, 4676 (1996).
- [22] V. Delgado and J. G. Muga, *Phys. Rev. A* **56**, 3425 (1997).
- [23] M. Razavy, *Il Nuovo Cimento B (1965-1970)* **63**, 271 (1969).
- [24] Y. Aharonov and D. Bohm, *Phys. Rev.* **122**, 1649 (1961).
- [25] G. R. Allcock, *Annals of Physics* **53**, 286 (1969).
- [26] S. Dhar, S. Dasgupta, and A. Dhar, *Journal of Physics A: Mathematical and Theoretical* **48**, 115304 (2015).
- [27] V. Dubey, C. Bernardin, and A. Dhar, *Phys. Rev. A* **103**, 032221 (2021).
- [28] H. Friedman, D. A. Kessler, and E. Barkai, *Physical Review E* **95**, 032141 (2017).
- [29] F. Thiel, E. Barkai, and D. A. Kessler, *Physical review letters* **120**, 040502 (2018).
- [30] W. Pauli, in *in Encyclopedia of Physics*, Vol. 5/1, edited by S. Flugge (Springer, Berlin, 1958) p. 60.
- [31] B. Misra and E. G. Sudarshan, *Journal of Mathematical Physics* **18**, 756 (1977).
- [32] G. C. Hegerfeldt, J. G. Muga, and J. Muñoz, *Phys. Rev. A* **82**, 012113 (2010).
- [33] J. Echanobe, A. Del Campo, and J. Muga, *Physical Review A—Atomic, Molecular, and Optical Physics* **77**, 032112 (2008).
- [34] N. Vona and D. Dürr, *The Message of Quantum Science: Attempts Towards a Synthesis*, 95 (2015).
- [35] S. Das, M. Nöth, and D. Dürr, *Phys. Rev. A* **99**, 052124 (2019).
- [36] D. S. Shucker, *Journal of Functional Analysis* **38**, 146 (1980).
- [37] S. Wolf and H. Helm, *Phys. Rev. A* **62**, 043408 (2000).
- [38] A. J. Bracken and G. F. Melloy, *Journal of Physics A: Mathematical and General* **27**, 2197 (1994).
- [39] H. F. Hofmann, *Phys. Rev. A* **96**, 020101 (2017).
- [40] S. Das, D.-A. Deckert, L. Kellers, S. Krekels, and W. Struyve, *arXiv preprint arXiv:2211.13362* (2022).
- [41] C. Kurtsiefer, T. Pfau, C. R. Ekstrom, and J. Mlynek, *Applied Physics B* **60**, 229 (1995).
- [42] R. I. Khakimov, B. Henson, D. Shin, S. Hodgman, R. Dall, K. Baldwin, and A. Truscott, *Nature* **540**, 100 (2016).
- [43] M. Allemand, R. Jannin, G. Dupuy, J.-P. Bureik, L. Pezzè, D. Boiron, and D. Clément, *PRX Quantum* **5**, 040324 (2024).
- [44] A. Bergschneider, V. M. Klinkhamer, J. H. Becher, R. Klemt, L. Palm, G. Zürn, S. Jochim, and P. M. Preiss, *Nature Physics* **15**, 640 (2019).
- [45] A. Omran, H. Levine, A. Keesling, G. Semeghini, T. T. Wang, S. Ebadi, H. Bernien, A. S. Zibrov, H. Pichler, S. Choi, *et al.*, *Science* **365**, 570 (2019).
- [46] R. Lopes, A. Imanaliev, A. Aspect, M. Cheneau, D. Boiron, and C. I. Westbrook, *Nature* **520**, 66 (2015).
- [47] A. Ayatollah Rafsanjani, M. Kazemi, V. Hosseinzadeh, and M. Golshani, *Scientific Reports* **14**, 3615 (2024).
- [48] J. D. Franson, *Physical review letters* **62**, 2205 (1989).
- [49] P. Sriftgiser, D. Guéry-Odelin, M. Arndt, and J. Dalibard, *Physical Review Letters* **77**, 4 (1996).
- [50] P. Ryczkowski, M. Barbier, A. T. Friberg, J. M. Dudley, and G. Genty, *Nature Photonics* **10**, 167 (2016).
- [51] M. Brown, S. Muleady, W. Dworschack, R. Lewis-Swan, A. Rey, O. Romero-Isart, and C. Regal, *Nature Physics* **19**, 569 (2023).
- [52] A. Tenart, G. Hercé, J.-P. Bureik, A. Dareau, and D. Clément, *Nature Physics* **17**, 1364 (2021).
- [53] R. Geiger and M. Trupke, *Physical Review Letters* **120**, 043602 (2018).
- [54] Y. Aharonov and D. Bohm, *Physical Review* **122**, 1649 (1961).
- [55] H. Paul, *Annalen der Physik* **464**, 252 (1962).
- [56] R. Giannitrapani, *International Journal of Theoretical Physics* **36**, 1575 (1997).
- [57] N. Grot, C. Rovelli, and R. S. Tate, *Phys. Rev. A* **54**, 4676 (1996).
- [58] I. L. Egusquiza and J. G. Muga, *Phys. Rev. A* **61**, 012104 (1999).
- [59] E. A. Galapon, *Journal of mathematical physics* **45**, 3180 (2004).
- [60] E. A. Galapon, *Proceedings of the Royal Society A: Mathematical, Physical and Engineering Sciences* **465**, 71 (2009).
- [61] E. A. Galapon, *Proceedings of the Royal Society of London. Series A: Mathematical, Physical and Engineering Sciences* **458**, 2671 (2002).
- [62] E. O. Dias and F. Parisio, *Physical Review A* **95**, 032133 (2017).
- [63] I. Egusquiza, J. Muga, B. Navarro, and A. Ruschhaupt, *Physics Letters A* **313**, 498 (2003).
- [64] C. Leavens, *Physics Letters A* **338**, 19 (2005).
- [65] C. Leavens, *Physics Letters A* **362**, 256 (2007).
- [66] M. Lienert, S. Petrat, and R. Tumulka, *Multi-time wave functions: An introduction* (Springer Nature, 2020).
- [67] D. Dürr and S. Teufel, in *Multiscale Methods in Quantum Mechanics: Theory and Experiment* (Springer, 2003) pp. 41–58.
- [68] M. A. Porras, A. Luis, and I. Gonzalo, *Physical Review A* **90**, 062131 (2014).
- [69] D. Burgarth, P. Facchi, H. Nakazato, S. Pascazio, and K. Yuasa, *Quantum* **4**, 289 (2020).
- [70] F. Thiel, I. Mualem, D. A. Kessler, and E. Barkai, *Physical Review Research* **2**, 023392 (2020).
- [71] F. Thiel, D. A. Kessler, and E. Barkai, *Physical Review A* **97**, 062105 (2018).
- [72] G. Allcock, *Annals of Physics* **53**, 311 (1969).

- [73] P. Facchi and S. Pascazio, *Physical review letters* **89**, 080401 (2002).
- [74] D. Home and M. Whitaker, *Annals of Physics* **258**, 237 (1997).
- [75] H. Nakazato, M. Namiki, and S. Pascazio, *International Journal of Modern Physics B* **10**, 247 (1996).
- [76] D. Georgiev, L. Bello, A. Carmi, and E. Cohen, *Phys. Rev. A* **103**, 062211 (2021).
- [77] J. Kofler, M. Singh, M. Ebner, M. Keller, M. Kotyrba, and A. Zeilinger, *Physical Review A* **86**, 032115 (2012).
- [78] A. Perrin, H. Chang, V. Krachmalnicoff, M. Schellekens, D. Boiron, A. Aspect, and C. I. Westbrook, *Physical review letters* **99**, 150405 (2007).
- [79] S. K. Lam, A. Pitrou, and S. Seibert, in *Proceedings of the Second Workshop on the LLVM Compiler Infrastructure in HPC* (2015) pp. 1–6.
- [80] T. Ono, Y. Tsujimoto, K. Wakui, and M. Fujiwara, *Scientific Reports* **14**, 1051 (2024).
- [81] R.-B. Jin, T. Gerrits, M. Fujiwara, R. Wakabayashi, T. Yamashita, S. Miki, H. Terai, R. Shimizu, M. Takeoka, and M. Sasaki, *Optics Express* **23**, 28836 (2015).
- [82] T. Gerrits, F. Marsili, V. B. Verma, L. K. Shalm, M. Shaw, R. Mirin, and S. W. Nam, *Physical Review A* **91**, 013830 (2015).
- [83] H. Yu, B. Crockett, N. Montaut, S. Sciara, M. Chemnitz, S. T. Chu, B. E. Little, D. J. Moss, Z. Wang, J. Azaña, *et al.*, *Physical Review Letters* **134**, 220801 (2025).
- [84] C. Kurtsiefer, T. Pfau, and J. Mlynek, *Nature* **386**, 150 (1997).
- [85] A. D. Cronin, J. Schmiedmayer, and D. E. Pritchard, *Rev. Mod. Phys.* **81**, 1051 (2009).
- [86] F. Anders, A. Idel, P. Feldmann, D. Bondarenko, S. Loriani, K. Lange, J. Peise, M. Gersemann, B. Meyer-Hoppe, S. Abend, *et al.*, *Physical Review Letters* **127**, 140402 (2021).
- [87] A. S. Abazi, R. Jaha, C. A. Graham-Scott, W. H. Pernice, and C. Schuck, *Physical Review Research* **7**, 033114 (2025).
- [88] A. Kawasaki, H. Brunel, R. Ide, T. Suzuki, T. Kashiwazaki, A. Inoue, T. Umeki, T. Yamashima, A. Sakaguchi, K. Takase, *et al.*, *Nature Photonics* **19**, 271 (2025).
- [89] G. B. Xavier, J.-Å. Larsson, P. Villoresi, G. Vallone, and A. Cabello, *npj Quantum Information* **11**, 129 (2025).
- [90] F. Roeder, R. Pollmann, M. Stefszky, M. Santandrea, K.-H. Luo, V. Quiring, R. Ricken, C. Eigner, B. Brecht, and C. Silberhorn, *PRX Quantum* **5**, 020350 (2024).
- [91] P. C. Flores and E. A. Galapon, *Phys. Rev. A* **105**, 062208 (2022).
- [92] D. R. Terno, *Physical Review A* **89**, 042111 (2014).
- [93] B. Rosenstein and M. Usher, *Physical Review D* **36**, 2381 (1987).
- [94] T. D. Newton and E. P. Wigner, *Reviews of Modern Physics* **21**, 400 (1949).
- [95] K. Kowalski and J. Rembieliński, *Physical Review A—Atomic, Molecular, and Optical Physics* **84**, 012108 (2011).
- [96] B. Rosenstein and L. Horwitz, *Journal of Physics A: Mathematical and General* **18**, 2115 (1985).
- [97] G. C. Hegerfeldt, *Physical review letters* **54**, 2395 (1985).
- [98] R. Wagner, M. Ware, E. Stefanovich, Q. Su, and R. Grobe, *Physical Review A—Atomic, Molecular, and Optical Physics* **85**, 022121 (2012).
- [99] C. T. Sebens, *Foundations of Physics* **49**, 365 (2019).
- [100] M. Kazemi and G. Jafari, *Quantum* **9**, 1904 (2025).
- [101] M. Kazemi, H. Hashamipour, and M. Barati, *Physical Review A* **98**, 012125 (2018).
- [102] T. Maudlin, *topoi* **14**, 7 (1995).
- [103] G. C. Ghirardi, A. Rimini, and T. Weber, *Physical review D* **34**, 470 (1986).
- [104] A. Bassi, K. Lochan, S. Satin, T. P. Singh, and H. Ulbricht, *Reviews of Modern Physics* **85**, 471 (2013).
- [105] D. Bohm, *Phys. Rev.(2)* **85**, 180 (1952).